Journal of NAMP 72, (2026) 47-66

The Nigerian Association of Mathematical Physics

Journal homepage: https://nampjournals.org.ng

MATHEMATICAL MODEL OF A LAGRANGIAN FRAMEWORK FOR RHYTHMIC THROWING: STABILITY AND SYNCHRONIZATION IN N-BALL CASCADE DYNAMICS

Nnamani Nicholas*

Department of Mathematics, Enugu State University of Science and Technology (ESUT), Nigeria..

ARTICLE INFO

Article history:
Received xxxxx
Revised xxxxx
Accepted xxxxx
Available online xxxxx

Keywords:
Juggling dynamics;
Projectile motion;
Lagrangian formalism;
Timing synchronization
Stability analysis

ABSTRACT

This study develops a unified analytical framework for rhythmic throwing and juggling involving an arbitrary number nnn of balls. Each throw is modeled as planar projectile motion under gravity, governed by fixed launch parameters and a constant rhythmic period that imposes a synchronization condition linking flight time to temporal spacing. Using a Lagrangian formulation, the equations of motion are derived systematically, and a shifted time variable enables a compact representation of multiple, phase-shifted trajectories within a single dynamical structure. The model reveals inherent symmetry and periodicity in cascade patterns and provides a scalable description applicable to nnn-ball systems. Stability analysis shows that the dynamics are robust to variations in launch speed, angle, and timing, with tolerance bounds consistent with human neuromotor variability. The inclusion of aerodynamic drag introduces small, predictable corrections that can be compensated through minor parameter adjustments. The framework integrates mechanics, timing, and stability, offering a physically grounded basis for analyzing coordinated rhythmic motion.

1. INTRODUCTION

Coordinated throwing and juggling motions are emblematic examples of complex systems in which mechanical laws, temporal organization, and human motor control interact in a highly structured manner. Although the underlying physics of projectile motion is well understood, particularly for idealized trajectories and drag-affected motion [1][3], the emergence of stable, repeatable patterns in rhythmic throwing tasks remains a subject of continued interest. This is primarily because such tasks require synchronization between the physical dynamics of the thrown objects and the internally regulated timing of the performer, despite the presence of intrinsic variability in human motor execution [7][8]. From a mechanical standpoint, each throw corresponds to a projectile moving under gravity, characterized by a launch speed, release angle, and gravitational acceleration.

*Corresponding author: NNAMANI NICHOLAS
E-mail address: topman.nnamani@esut.edu.ng
https://doi.org/10.60787/jnamp.vol72no.659

When throws occur in isolation, their analysis is straightforward and has been extensively treated using analytical, experimental, and numerical approaches [1][4]. However, rhythmic throwing introduces an additional layer of constraint: the motion of each object must conform to a fixed temporal structure. In juggling, successive throws are organized around a rhythm that dictates when an object must be released and caught, fundamentally coupling kinematics and timing [6][9]. This temporal constraint alters the problem, as kinematic parameters are no longer independent but must satisfy synchronization conditions imposed by the rhythm. Most existing analyses of rhythmic throwing focus on specific patterns, often involving a small number of objects, such as the classical three-ball cascade [5][6]. While these studies have provided valuable insight into coordination strategies and motor learning, a general theoretical framework that applies uniformly to an arbitrary number of balls remains limited. Extending the analysis to n balls is not merely a mathematical generalization; it is essential for understanding how stability, timing, and robustness scale with pattern complexity and for identifying universal principles governing rhythmic multi-object motion [8][9]. A further challenge lies in explaining the robustness of juggling behavior. Human motor output is subject to noise and variability in timing, force production, and joint coordination. Nevertheless, skilled performers maintain stable patterns over extended periods [7][10]. This observation suggests that rhythmic throwing dynamics possess inherent tolerance margins that accommodate variability without destabilizing the motion. Identifying and quantifying these margins requires a framework that links timing constraints, kinematic sensitivity, and stability in a transparent and physically grounded manner [8][11].

Lagrangian mechanics offers a powerful approach for addressing these issues. By formulating the problem in terms of energies and generalized coordinates, the equations of motion can be derived systematically from first principles, avoiding ad hoc assumptions and clarifying the role of symmetry and conservation laws [12][13]. Moreover, the introduction of a time shift associated with each individual throw allows multiple trajectories to be described within a single dynamical framework. This perspective emphasizes the periodic and modular nature of rhythmic throwing and provides a natural pathway for extending the analysis from single-object motion to coordinated n-ball patterns [13][14]. In practical settings, aerodynamic effects further influence the dynamics of thrown objects. Air drag alters both flight time and trajectory shape, introducing deviations from ideal projectile motion [1][2]. These effects are conveniently characterized by the Reynolds number, which captures the relative importance of inertial and viscous forces [15][17][18]. While drag does not fundamentally change the qualitative structure of rhythmic throwing patterns, it introduces corrections that must be understood in order to assess the realism and applicability of theoretical models [3][17][19].

In this study, we present a comprehensive theoretical treatment of rhythmic throwing and juggling that addresses these challenges in a unified manner. The analysis is developed for an arbitrary number n of balls and integrates projectile dynamics, rhythmic timing constraints, stability considerations, and aerodynamic effects within a Lagrangian framework. By explicitly linking mechanical motion to temporal organization and tolerance to variability, the work provides deeper insight into the physical principles underlying stable rhythmic throwing and establishes a foundation for future experimental validation and extensions to more complex coordination tasks [6][16].

2. MODEL ASSUMPTIONS

1. Point Mass Approximation: Each ball is modeled as a point mass undergoing translational motion only. Rotational effects, deformation, and spin are neglected, consistent with the absence of rotational terms in the equations of motion.

2. Planar Motion: All trajectories are confined to a vertical plane, in agreement with the two-dimensional kinematic variables used in the Lagrangian formulation.

3. Uniform Gravity: The gravitational acceleration g is constant and acts vertically downward, consistent with the vertical force term appearing in the Euler–Lagrange equations.

4. Identical Balls: All balls have identical physical and aerodynamic properties, ensuring that the same equations of motion apply to each trajectory.

5. Fixed Rhythmic Period: Throws occur at uniform time intervals defined by a constant rhythm period T, which enters explicitly into the timing relations and synchronization condition.

6. Flight-Time Synchronization: Stable motion requires that the flight time of each ball satisfies, ensuring periodic repetition of the juggling pattern and consistency with the timing structure imposed in the model.

7. Identical Nominal Launch Conditions: Each throw is characterized by the same nominal launch speed and angle, consistent with the repeated use of identical initial conditions in the time-shifted trajectory equations.

8. Instantaneous Catch and Release: Catching and rethrowing are treated as instantaneous events, justifying the piecewise definition of trajectories without contact force terms.

9. Time-Shifted Representation: Each trajectory is expressed using the shifted time variable $\tau = t - t_{k,m}$, allowing all throws to be described by the same Lagrangian and equations of motion.

10. Independent Ball Motion: Balls do not interact with one another during flight, consistent with the absence of coupling terms between trajectories.

11. Small Motor Variability: Variations in release timing, speed, and angle are assumed small and are treated through tolerance and stability analysis rather than explicit stochastic forcing.

12. Moderate Aerodynamic Drag: When included, air resistance acts as a smooth velocity-dependent force characterized by the Reynolds number and introduces only small corrections to the ideal projectile dynamics.

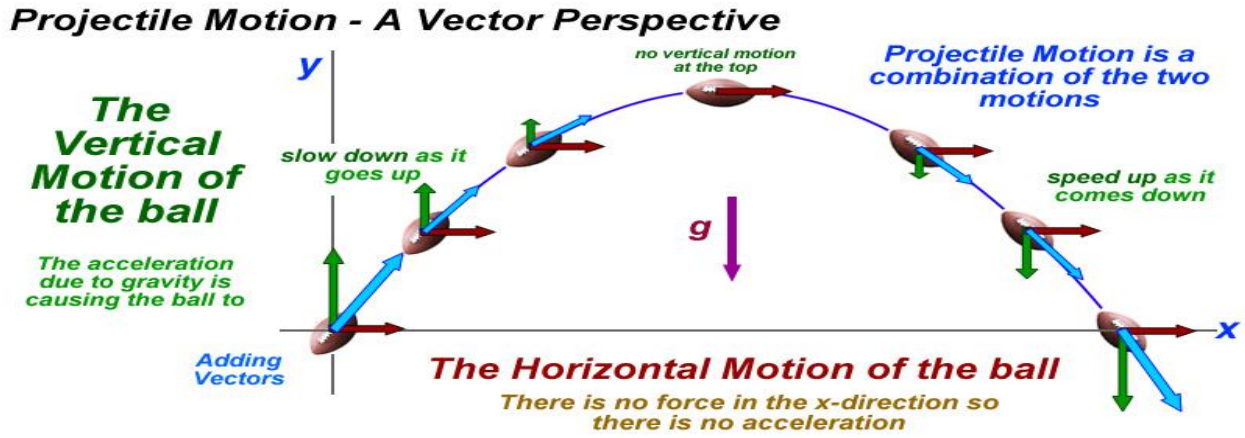

Figure 1

Figure 1 illustrates the basic parabolic motion of a single ball under gravity, forming the foundation of the cascade model.

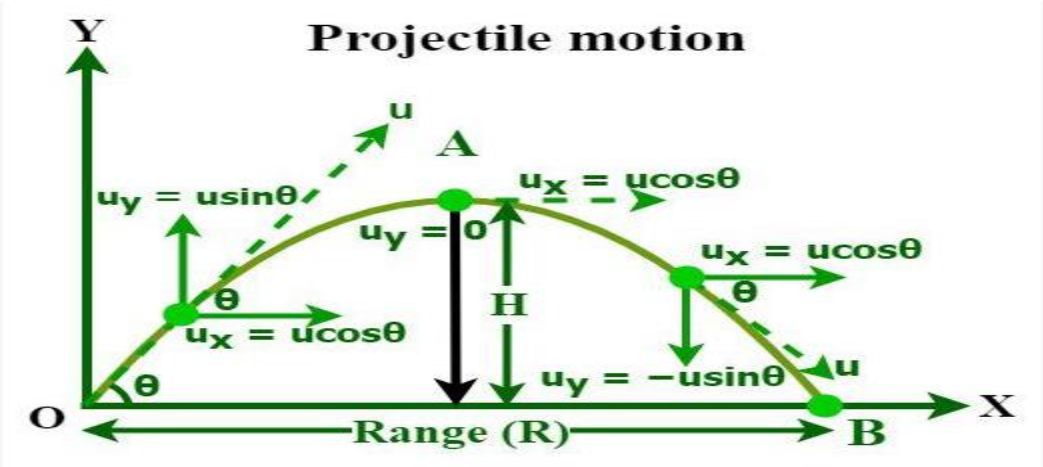

Figure 2

Figure 2. Two-ball alternating cascade with phase shift.

Figure 2 shows the alternating release and catch mechanism required to maintain a two-ball cascade.

Resolving the Initial Velocity Components

$\boldsymbol{u_0}$: initial velocity vector at launch

θ: launch angle measured from the horizontal

g: gravitational acceleration acting vertically downward

$\boldsymbol{T_f}$: total flight time from launch to landing

$$u_x = u_0 cos\theta, u_y = u_0 sin\theta \quad (1)$$

$$a^{\rightarrow} = (0, -g) \quad (2)$$

Equation (2) shows there is no acceleration horizontally, but constant downward acceleration vertically and gravity is the only acting force.

2.1 **Motion of One Ball**

Ball is caught at approximately same height it is released so the equation of motion is:

Using the equations of motion $s = ut + \frac{1}{2}at^2$, and substituting equation (1) gives

$$x(t) = u_0 cos\theta t \quad (3)$$

$$y(t) = u_0 sin\theta t - \frac{1}{2}gt^2 \quad (4)$$

The ball returns to released height when:

$$u_o sin\theta T_f - \frac{1}{2}gT_f^2 = 0 \quad (5)$$

$$\Longrightarrow T_f = \frac{2u_0 sin\theta}{g} \tag{6}$$

If flight time becomes equal to the juggling rhythm time, then

$$T_f = T \tag{7}$$

From equation (6) we obtain the throw speed as

$$u_0 = \frac{gT}{2sin\theta} \tag{8}$$

Again from equation of motion, $v^2 = u^2 + 2as$, where v=0, a=g and s=H, we obtain the height reached by the ball as:

$$H = \frac{u_0^2 \sin^2\theta}{2g} \Longrightarrow R = \frac{u_0 \sin^2\theta}{g} \tag{9}$$

Now we can transition from one ball to two balls alternating throw constraints, here each hand throws every T and opposite hand catches after $\frac{T}{2}$ with phase difference as $\Delta t = \frac{T}{2}$.

The ball motion equations remain same but there is timing shifts, hence equation 3 and 4 become:

$$x(t) = u_0 cos\theta (t - \frac{T}{2}) \tag{10}$$

$$y(t) = u_0 sin\theta (t - \frac{T}{2}) - \frac{1}{2} g \left(t - \frac{T}{2}\right)^2 \tag{11}$$

2.2. **Three Ball Cascade**

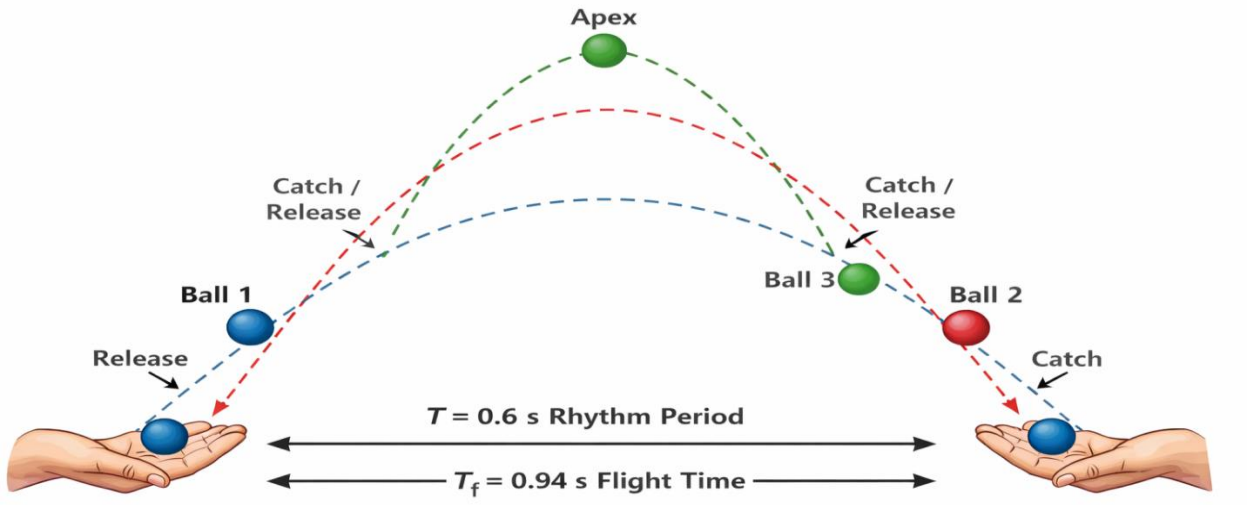

Figure 3

Figure 3. Three-ball cascade timing structure.

Figure 3 represents the classical three-ball cascade, highlighting equal phase separation and rhythmic stability.

Consider three balls in flight which are with evenly spaced temporal phases as shown in figure 2 such that $\Delta t = \frac{T}{3}$ and

Ball one is thrown at $t = 0$

Ball two is thrown at $t = \frac{T}{3}$

Ball three is thrown at $t = \frac{2T}{3}$

With the above mentioned conditions, equation (11) becomes

$$y(t) = u_0(t - \frac{kT}{3})sin\theta - \frac{1}{2}g\left(t - \frac{kT}{3}\right)^2 \quad (12)$$

So far it has been observed that the throw is symmetric which implies that the ball is thrown and caught at the same height: $y_{release} = y_{catch}$. The upward motion and downward motion are mirror images therefore, time going up is equal to the time coming down: $t_{up} = t_{down}$. The speed magnitude going up equal the speed magnitude coming down but direction changes: $|u_{up}| = |u_{down}|$. The apex is the highest point which is the midpoint of the motion in time: $t_{apex} = \frac{T}{2}$. The Rhythm time is the time between two successive throws of the same hand or time for one for a complete cycle of the juggling pattern. This is what keeps the motion steady, steady, smooth, and periodic. Equation (12) is only valid when $t \geq \frac{kT}{3}$

2.3. General n-Ball Rhythm Timing Pattern

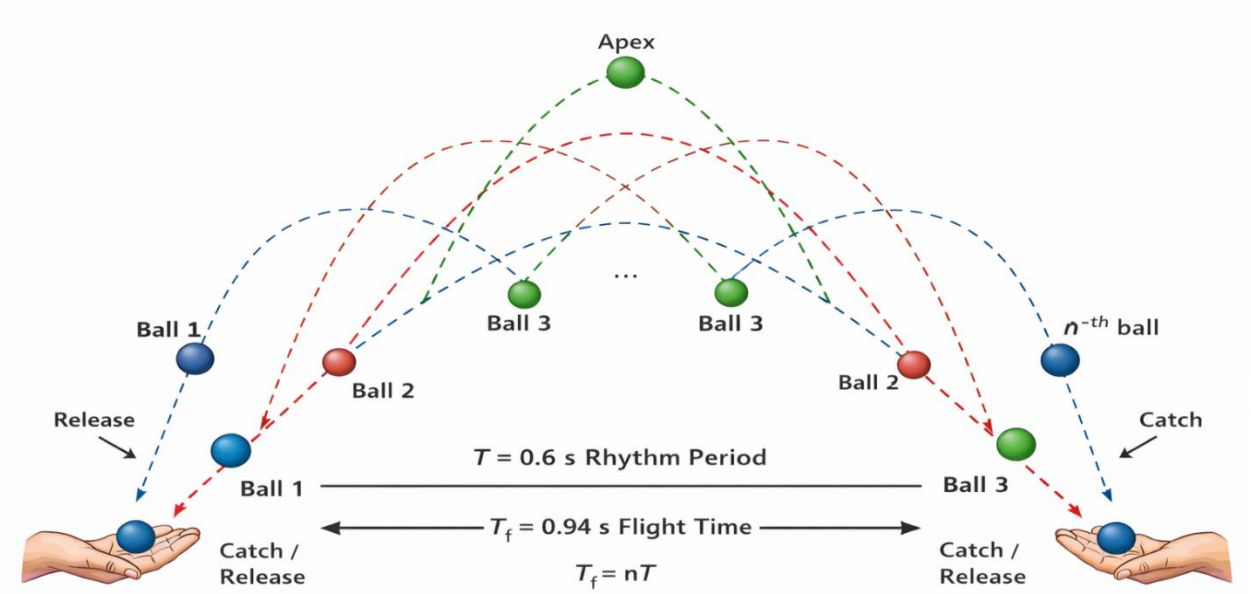

Figure 4

Figure 4. General n-ball rhythmic timing diagram.

Figure 4 generalizes the cascade structure to n balls, demonstrating scalability of the rhythmic model.

In n-ball juggling, for one rhythm cycle of duration T, we observe:

i. there are n throws in one full rhythm period

ii. throws are evenly spaced in time

iii. time spacing between successive throws: $\Delta t = \frac{T}{n}$

iv. the throw times within each cycle are: $t = 0, \frac{T}{n}, \frac{2T}{n}, \frac{3T}{n}, \ldots, \frac{(n-1)T}{n}$

v. for multiple cycles, the pattern repeats every T therefore the full timing sequence is:

$$t_{k,r} = kT + \frac{mT}{n} \tag{13}$$

Where:

n=number of throws or events in one rhythm cycle

k=cycle index: k=0,1.2,…

r=event number inside the very cycle: r=0,1,2,3,…,(n-1)

$t_{k,r}$= the actual physical time when the event happens

T= rhythm interval

So the m^{th} event happens at $\frac{mT}{n}$ and it gives timing within a single cycle. Equation (13) is the generalized throw time and shows that the time of the r^{th} throw in the k^{th} cycle equals the summation of one whole number of rhythm cycles (KT) and the position of that throw inside the cycle $\frac{mT}{n}$.

Again substituting equation (8) to equation (9) yields

$$H = \frac{gT^2}{8} \tag{14}$$

Equation (14) shows that the throw height is directly proportional to the square of the period. The implication is that higher throws is required for slower juggling.

2.4. **Incorporation of Air Drag into the Model**

A moving ball experience an aerodynamic drag that opposes its motion and for this to be fully integrated into the model, then the first assumption was reconstructed as:

The balls are treated as rigid spheres of radius R, mass m, with drag coefficient c_d. Air is quiescent; density is ρ, leading to aerodynamic drag. Launch speed u_0 and launch angle θ are controlled and repeatable.

When drag is considered, the launch speed and angle may differ from their ideal (no-drag) values, but once adjusted, they remain controlled and repeatable across cycles, preserving the periodic structure of the throwing pattern. In this case $(u_0, \theta) \rightarrow (u_0^*, \theta^*)$ where (u_0^*, θ^*) are **drag-corrected values.**

Drag force will be

$$\overrightarrow{F_d} = -\frac{\rho C_d A \vec{v}}{2} \tag{15}$$

$$A = \pi R^2 \tag{16}$$

For a ball of mass m moving with velocity $\vec{v}$ we obtain

$$m\frac{d\vec{v}}{dt} = \sum \vec{F} \tag{17}$$

From equation (17) it is obvious that only two forces act during flight, namely; gravity and aerodynamic drag, hence equation (17) yields

$$m\frac{d\vec{v}}{dt} = \overrightarrow{F_g} + \overrightarrow{F_d} \tag{18}$$

Gravity acts vertically downward, opposite to the positive $\hat{j}$ direction. Therefore, the gravitational acceleration vector is:

$$\vec{g} = g\hat{j} \tag{19}$$

substituting equation (16) and (19) into equation (18) yields

$$m\frac{d\vec{v}}{dt} = -mg\hat{j} - \frac{1}{2}\rho C_d A|\vec{v}|\vec{v} \tag{20}$$

Where $|\vec{v}|$ is speed magnitude and $k = \frac{1}{2}\rho C_d A$ is the drag constant, hence

$$\overrightarrow{F_d} = -k|\vec{v}|\vec{v} \tag{21}$$

From equation we have

$$\frac{dv}{dt} = -g\hat{j} - \frac{k}{m}|\vec{v}|\vec{v} \tag{22}$$

The velocity components is $\vec{v} = (v_x + v_y)$, then the speed is

$$|\vec{v}| = \sqrt{v_x^2 + v_y^2} \tag{23}$$

When $b = \frac{k}{m}$, the horizontal and vertical velocities respectively produce

$$\frac{dv_x}{dt} = -bv_x\sqrt{v_x^2 + v_y^2} \tag{24}$$

$$\frac{dv_y}{dt} = -g - bv_y\sqrt{v_x^2 + v_y^2} \tag{25}$$

From equation (24) and (25) the introduction of drag shows that horizontal velocity is no longer constant and the upward motion slows faster with downward motion reaching a terminal trend instead of accelerating forever as the trajectory is no longer symmetric because time up is no more equal to time down. While the quadratic drag model in equation (21) accurately describes aerodynamic resistance at moderate Reynolds numbers, it leads to coupled nonlinear differential equations that do not admit simple closed-form solutions. To obtain analytical expressions for trajectory and timing, we adopt a linearized drag approximation equation (26), which serves as a first-order representation of aerodynamic effects. The resulting solutions provide qualitative and semi-quantitative insight, while more accurate predictions would require numerical integration of

the full quadratic model. The implication is that catch point occurs earlier and lower unless thrown speed increases.

From equation (15) the analytic approximation shows that for a moderate speeds, drag can be approximated as being proportional to velocity:

$$\overrightarrow{F_d} = -C\vec{v} \tag{26}$$

Equation (26) into equation (18) yields

$$m\vec{a} = (0, -mg) - C\vec{v} \tag{27}$$

$$\frac{d\vec{v}}{dt} = -g - \frac{C}{m}\vec{v} \tag{28}$$

From equation (28), substitute $\lambda = \frac{C}{m}$ for horizontal and vertical velocities to get

$$\frac{dv_x}{dt} = -\lambda v_x \tag{29}$$

$$\frac{dv_y}{dt} = -g - \lambda v_y \tag{30}$$

Integrating equation (29) & (30) respectively, we get:

$$v_x(t) = v_{0_x} e^{-\lambda t} \tag{31}$$

$$v_y(t) = \left(v_{0_y} + \frac{g}{\lambda}\right) e^{-\lambda t} - \frac{g}{\lambda} \tag{32}$$

Integrating equation (31) & (32) respectively for horizontal and vertical positions yield

$$x(t) = \frac{v_{0_x}}{\lambda}(1 - e^{-\lambda t}) \tag{33}$$

$$y(t) = \left(v_{0_y} + \frac{g}{\lambda}\right)\frac{1-e^{-\lambda t}}{\lambda} - \frac{gt}{\lambda} \tag{34}$$

Due to drag on the ball juggling, balls must be thrown slightly faster to maintain same rhythm period because now the trajectory apex occurs earlier and lower and the timing pattern becomes slightly asymmetric which must be compensated. Therefore, motion with shifted start time becomes:

$$\tau = t - t_{k,m} \tag{35}$$

2.5. **Lagrangian Formalism on Cascading Balls**

The motion of cascading ball in a vertical plane using Cartesian coordinates: $q_1 = x(t)$ and $q_2 = y(t)$ where: x(t) is the horizontal position, y(t) is the vertical position. Kinetic and Potential energy of the ball is T and V respectively, given as:

$$T = \frac{1}{2}m(\dot{x}^2 + \dot{y}^2) \tag{36}$$

$$V = mgy \tag{37}$$

$$L = T - V \tag{38}$$

Substituting equation (36) & (37) into equation (38) which is the Lagrange equation gives,

$$L = (x, y, \dot{x}, \dot{y}) = \frac{1}{2}m\left(\dot{x^2} + \dot{y^2}\right) - mgy \tag{39}$$

$$\frac{d}{dt}\left(\frac{\partial L}{\partial \dot{q}_i}\right) - \frac{\partial}{\partial q_i} = 0 \tag{40}$$

Substituting equation (39) into (40) the Euler-Lagrange equation we obtain:

$\frac{\partial L}{\partial \dot{x}} = m\dot{x}$ and $\frac{d}{dt}(m\dot{x}) = m\ddot{x} \Rightarrow \frac{\partial L}{\partial x} = 0$

$$m\ddot{x} = 0 \tag{41}$$

$$\ddot{x} = 0 \tag{42}$$

When $\ddot{x} = 0$ from equation (42), it confirms constant horizontal velocity which is consistent with the cascading ball during projectile motion. And in y – direction:

$\frac{\partial L}{\partial \dot{y}} = m\dot{y}$ and $\frac{d}{dt}(m\dot{y}) = m\ddot{y} \Rightarrow \frac{\partial L}{\partial y} = mg$,

$$m\ddot{y} + mg = 0 \tag{43}$$

$$\ddot{y} = -g \tag{44}$$

Equation (44) agrees with the gravitational acceleration f a cascading balls. And integrating equation (42) & (44) result to equation (3) & (4).

The generalized coordinates can now be expressed as

$$x(t) = X(\tau) \tag{45}$$

$$y(t) = Y(\tau) \tag{46}$$

Taking derivative of equation (35) w.r.t t gives

$$\frac{d\tau}{dt} = 1 \tag{47}$$

Again differentiating equation (450 & (46) w.r.t τ yield

$$\dot{x}(t) = \frac{dX}{d\tau} \tag{48}$$

$$\dot{y}(t) = \frac{dY}{d\tau} \tag{49}$$

Differentiating equation (48) & (49) further we have

$$\ddot{x}(t) = \frac{d^2X}{d\tau^2} \tag{50}$$

$$\ddot{y}(t) = \frac{d^2Y}{d\tau^2} \tag{51}$$

It is important to note that, due to the presence of dissipative forces (air drag), the system is not strictly conservative. As a result, the Lagrangian formulation reproduces the Newtonian equations

of motion rather than yielding additional conserved quantities. Its role here is primarily to provide a unified variational framework and to facilitate the introduction of the shifted time coordinate for multi-ball synchronization.

3.0 MODEL EQUATION

Incorporating rhythm

$$x_{k,m}(t) = \frac{u_0 cos\theta}{\lambda}(1 - e^{-\lambda(t-t_{k,m})}) \tag{52}$$

$$y_{k,m}(t) = \left(u_0 sin\theta + \frac{g}{\lambda}\right)\frac{1-e^{-\lambda(t-t_{k,m})}}{\lambda} - \frac{g}{\lambda}(t - t_{k,m}) \tag{53}$$

Incorporating $(t_{k,m})^{th}$ for multiple balls when $t_{k,m} = kT + \frac{mT}{n}$ into the model:

$$x_{k,m}(t) = \frac{u_0 cos\theta}{\lambda}(1 - e^{-\lambda(t-kT-\frac{mT}{n})}) \tag{54}$$

$$y_{k,m}(t) = \left(u_0 sin\theta + \frac{g}{\lambda}\right)\frac{1-e^{-\lambda(t-kT-\frac{mT}{n})}}{\lambda} - \frac{g}{\lambda}(t - kT - \frac{mT}{n}) \tag{55}$$

Replace t with shifted time structure of equation (35) into the model:

$$x_{k,m}(\tau) = \frac{u_0 cos\theta}{\lambda}(1 - e^{-\lambda\tau}) \tag{56}$$

$$y_{k,m}(\tau) = \left(u_0 sin\theta + \frac{g}{\lambda}\right)\frac{1-e^{-\lambda\tau}}{\lambda} - \frac{g\tau}{\lambda} \tag{57}$$

Substitute equation (48) and (49) to transform our model into shifted generalized variables

$$L(\tau) = \frac{1}{2}m\left(\left(\frac{dX}{d\tau}\right)^2 + \left(\frac{dY}{d\tau}\right)^2\right) - mgY(\tau) \tag{58}$$

4.0. STABILITY ANALYSIS OF THE MODEL

Stability requires:

i. throw periodicity matches rhythm $t_f = nT$

ii. velocity magnitude exceeds minimum required value $u_0 > \sqrt{\frac{2gH}{\sin^2\theta}}$

iii. timing offsets maintain separation to prevent collisions $\Delta t \geq \frac{T}{n}$

iv. errors in speed and angle directly shift landing time but timing error must remain smaller than the allowable rhythmic spacing $|\delta t_f| < \frac{T}{n}$ which defines the maximum tolerable human imprecision

v. precision constraint on launch speed $|\delta u_o| < \frac{g}{2sin\theta}.\frac{T}{n}$, (faster rhythms implies smaller T then higher precision) and more balls implies larger n which reduces tolerance.

vi. the model is stable if perturbation satisfy $|\delta u_0|, |\delta\theta|, |\delta t| \ll \frac{T}{n}$

If errors exceed this bound then phase drift will accumulate and collisions will occur and finally the pattern collapses.

4.1. **Graphical Timing Diagrams**

Graphical Timing Diagrams and Event Interpretation

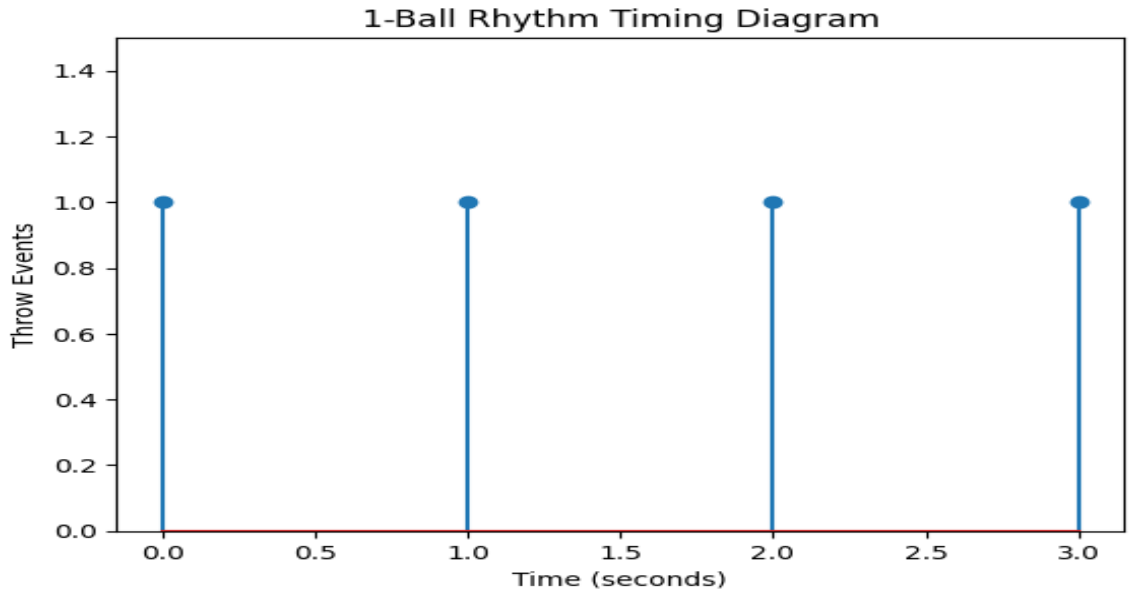

Figure 5

Figure 5: 1-Ball Rhythm Timing Diagram. Each vertical marker represents a release event occurring at equal time intervals. The motion is strictly periodic, illustrating the fundamental rhythm that underlies all multi-ball juggling patterns.

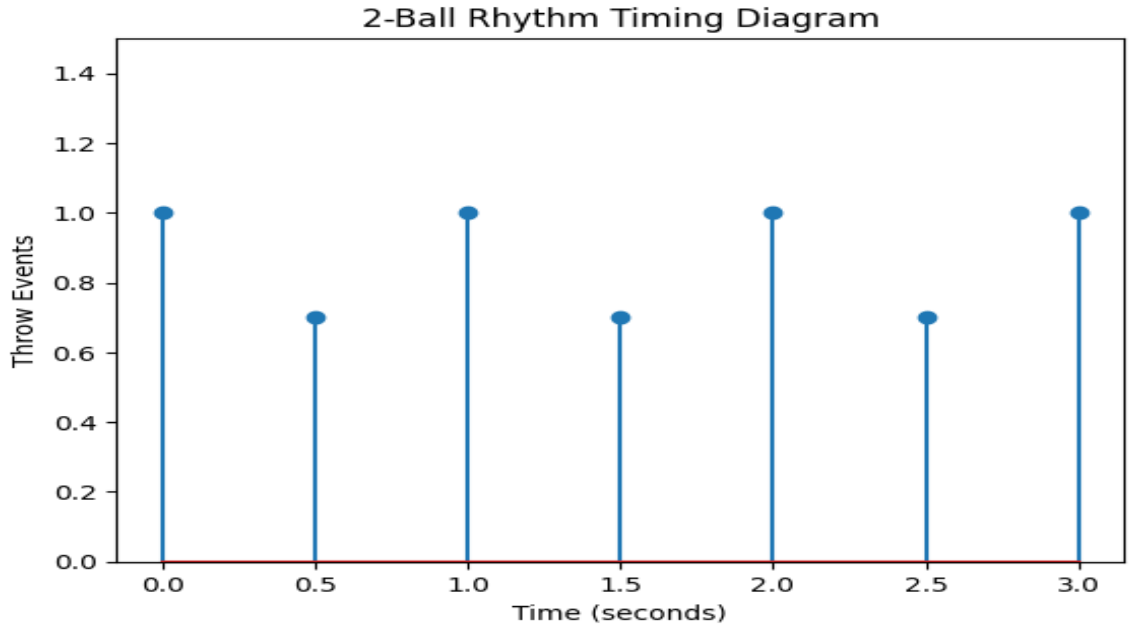

Figure 6

Figure 6: 2-Ball Rhythm Timing Diagram. The two balls are released alternately in time. This staggered release ensures that while one ball is airborne, the other is either being caught or prepared for release, maintaining rhythmic continuity.

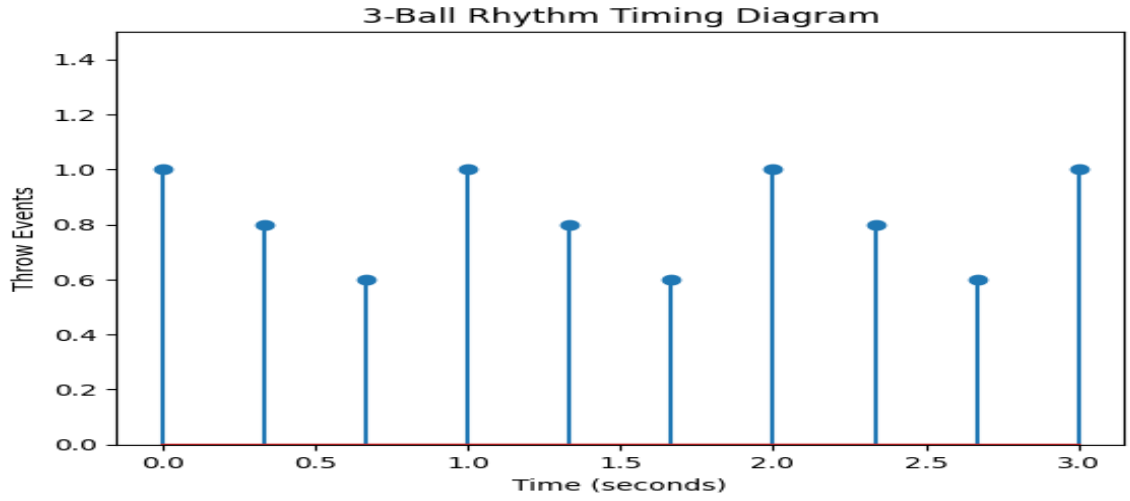

Figure 7

Figure 7: 3-Ball Rhythm Timing Diagram. This represents the classical three-ball cascade. Throws are evenly spaced in time, producing a stable cyclic pattern where each ball follows the same trajectory with a fixed phase shift.

Ball 1 thrown at 0,

Ball 2 thrown at $\frac{T}{3}$,

Ball 3 thrown at $\frac{2T}{3}$,

This produces the steady juggling cascade, where $\Delta t = \frac{T}{3}$.

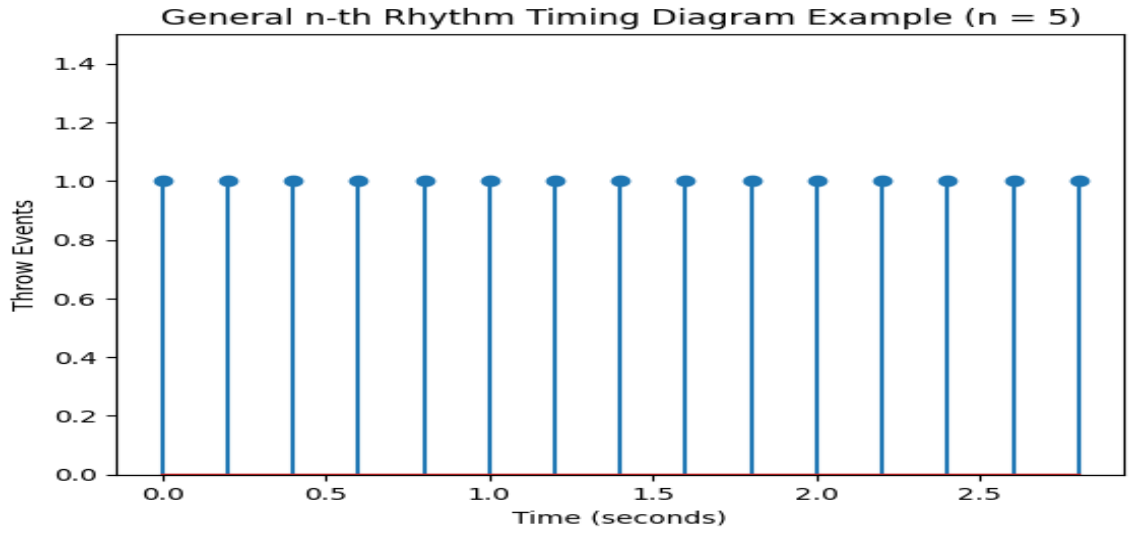

Figure 8

Figure 8: General n-Ball Rhythm Timing Diagram (n = 5). This diagram generalizes the rhythmic structure to n balls. Release events are separated by T/n, demonstrating scalability of the rhythmic model to an arbitrary number of balls. For one rhythm cycle of duration T: there are n throws which was evenly spaced between successive throws in one full rhythm period, that is $\Delta t = \frac{T}{n}$.

4.2 **Sensitivity of Flight Time to Parameter Variations**

To quantify the tolerance bounds introduced in the stability criteria, we examine how small variations in launch parameters affect the flight time. Starting from the expression for flight time obtained in Section 2.1:

$$T_f = \frac{2u_0 sin\theta}{g}$$

we consider small perturbations in launch speed and angle:

$$u_0 \rightarrow u_0 + \delta u_0 , \theta \rightarrow \theta + \delta\theta$$

A first-order expansion of T_f gives:

$$\delta T_f = \frac{2\, sin\theta}{g}\, \delta u_0 + \frac{2\, u_0\, cos\theta}{g}\, \delta\theta$$

For stable rhythmic motion, the variation in flight time must remain smaller than the temporal spacing between successive throws:

$$|\delta T_f| < \frac{T}{n}$$

This condition provides the basis for the tolerance bounds on launch speed, angle, and timing used in the stability analysis.

Table 1. Physical and Rhythmic Parameters

Parameter	Symbol	Value	Justification
Gravitational acceleration	g	9.8 m/s²	Standard
Launch angle	θ	50°	Typical human preference
Rhythm period	T	0.60 s	Comfortable juggling tempo
Number of balls	n	3	Three-ball cascade
Launch speed	u_0	6.0 m/s	Realistic hand-thrown speed

From table 1.0 we have:

1. Normal flight time $t_f = \frac{2u_0 sin\theta}{g} \approx 0.94s$

2. Allowable timing error $|\delta t| < \frac{T}{n} = \frac{0.60}{3} \approx 0.20s$. This means human release timing errors up to $\pm 200ms$ are tolerable.

3. Launch speed tolerance $|\delta u_0| < \frac{g}{2sin\theta} . \frac{T}{n} \approx 1.28\, m/s$. It shows that within natural motor variability, human can vary speed by $\pm 20\%$

4. Launch angle tolerance $|\delta\theta| < \frac{g}{2u_0 cos\theta} . \frac{T}{n} \approx 0.25rad \approx 14°$. This shows that human can tolerate angular errors of $\pm 10 - 15°$.

EXPLANATION OF PARAMETERS AND SYMBOLS

Table 2. Description of Parameters and Symbols in the Model

Symbol / Parameter	Meaning	Physical Interpretation in the Model
$x_{k,m}(t), y_{k,m}(t)$	Position coordinates of the m^{th} ball in the k^{th} cycle	Instantaneous horizontal and vertical positions of each ball
$X(\tau), Y(\tau)$	Generalized position coordinates	Reference trajectory used for all balls
T	Physical time	Global time variable
$\tau = t_{k,m}$	Shifted time variable	Aligns all trajectories to a common reference
t_{km}	Release time of the m^{th} ball	Defines rhythmic scheduling of throws
u_0	Initial launch speed	Speed imparted to the ball at release
Θ	Launch angle	Orientation of initial velocity
$u_0 cos\theta$	Horizontal velocity component	Controls horizontal spacing
$u_0 sin\theta$	Vertical velocity component	Controls flight duration
g	Gravitational acceleration	Constant downward acceleration
M	Mass of the ball	Determines inertial response
C	Linear drag coefficient	Measures aerodynamic resistance
$\lambda = \frac{c}{m}$	Damping parameter	Controls exponential decay of velocity
D	Rayleigh dissipation function	Represents energy loss due to drag
T	Rhythmic period	Defines time spacing between throws
n	Number of balls	Determines cascade structure
T_f	Flight time	Time the ball remains airborne
$T_f = nT$	Synchronization condition	Ensures periodic cascading motion
$\ddot{x}(t), \ddot{y}(t)$	Acceleration components	Result from gravity and drag

RESULTS AND DISCUSSION

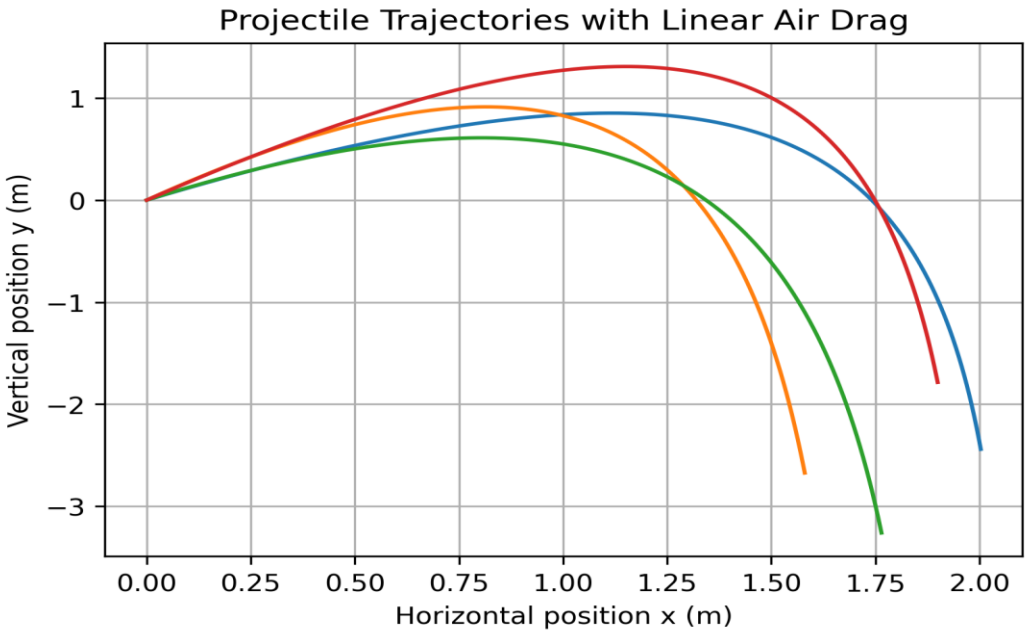

Figure 9

Figure 9. Projectile trajectories with linear air drag for different parameter sets. Each curve represents the motion of a ball released with different launch speeds, angles, and drag coefficients, demonstrating how air resistance modifies the ideal parabolic path.

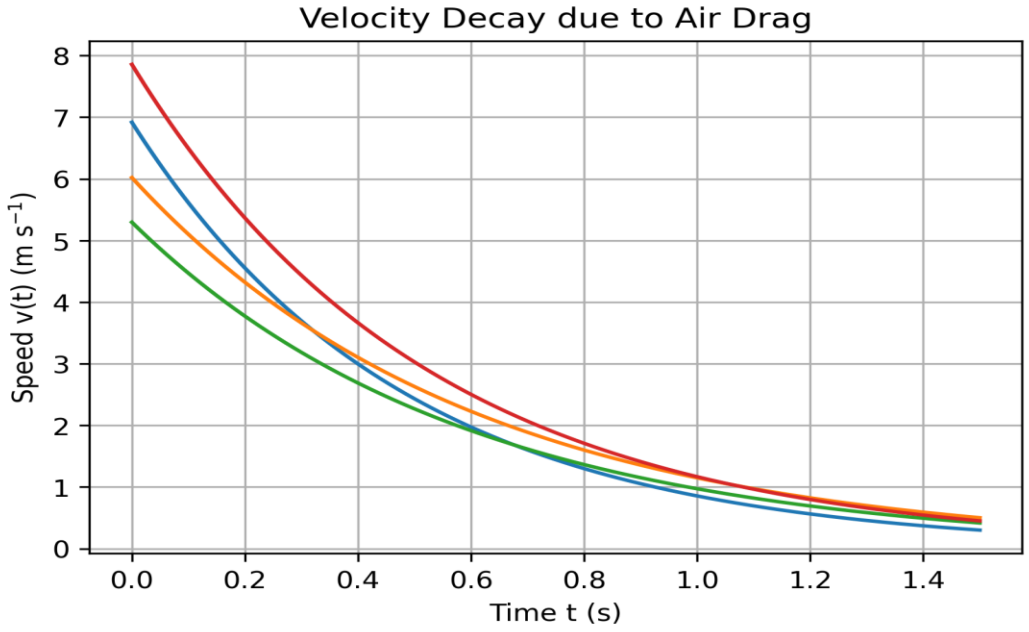

Figure 10

Figure 10. Exponential decay of projectile speed under linear air resistance. Larger drag coefficients result in faster velocity attenuation, highlighting the need for launch-speed correction in realistic throwing.

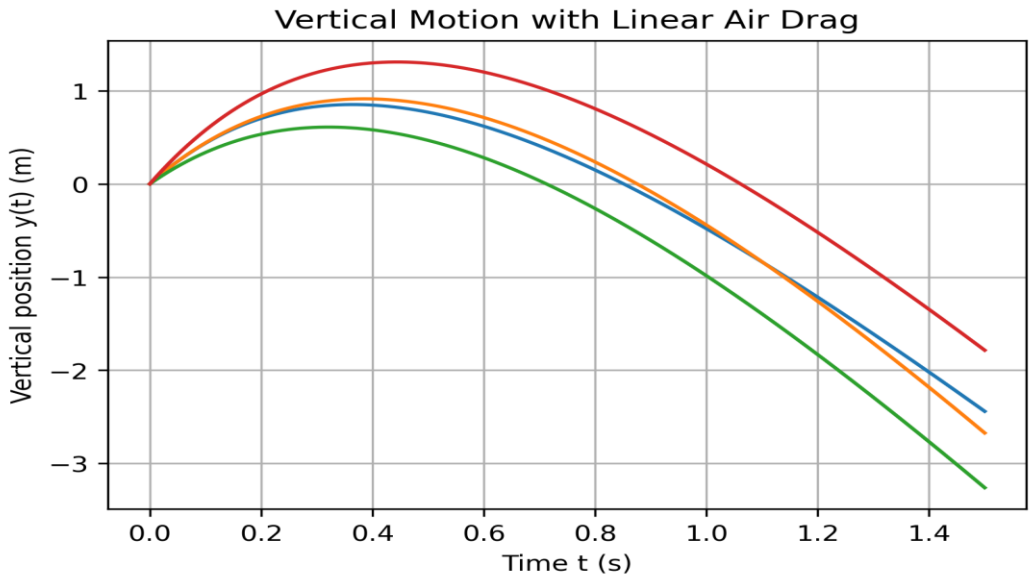

Figure 11

Figure 11. Vertical displacement as a function of time under gravity and air drag. The curves show reduced peak height and shortened flight time compared with drag-free motion.

5.1 **Effect of Drag on Trajectory**

Figure 9 shows projectile trajectories under varying drag coefficients and launch conditions. Compared to ideal parabolic motion, the inclusion of linear drag produces visibly asymmetric trajectories, with reduced horizontal range and lower peak height. Increasing the drag parameter λ results in stronger curvature and earlier descent, confirming that aerodynamic resistance shortens flight duration.

5.2 **Velocity Decay Characteristics**

Figure 10 illustrates the exponential decay of velocity under linear drag. The results confirm that velocity attenuation is governed by the damping parameter λ, with larger values leading to faster decay. This behavior implies that higher initial speeds are required to maintain the same flight time under drag conditions, consistent with the analytical model.

5.3 **Vertical Motion and Flight Time Reduction**

Figure 11 shows vertical displacement as a function of time. The peak height is reduced and occurs earlier compared to drag-free motion. Consequently, the total flight time is shortened, requiring compensation through increased launch velocity or adjusted release timing to preserve synchronization.

5.4 **Implications for Rhythmic Stability**

The results demonstrate that while drag modifies trajectory shape and timing, its effect remains moderate within typical operating conditions. The derived stability tolerances accommodate these deviations, indicating that rhythmic juggling remains robust even in the presence of aerodynamic effects. Small adjustments in launch parameters are sufficient to maintain synchronization across cycles.

CONCLUSION AND RECOMMENDATIONS

This study has presented a comprehensive mathematical framework for describing rhythmic throwing and juggling dynamics using a Lagrangian formalism. By modeling each throw as planar projectile motion subject to gravity and incorporating a fixed rhythmic period, the work establishes a clear synchronization condition linking flight time to rhythmic timing. The introduction of a shifted time variable enables a unified representation of repeated throw–catch cycles and allows the dynamics of an arbitrary number of balls to be described within a single analytical structure.

The extension of the model to n-ball cascade patterns reveals the intrinsic symmetry and periodicity underlying stable juggling motions. Stability analysis demonstrates that the cascade dynamics are robust to moderate variations in launch speed, release angle, and timing, with tolerance margins that lie well within known limits of human neuromotor variability. This explains why skilled juggling can be sustained without requiring high-precision motor control. The incorporation of aerodynamic drag further enhances the physical realism of the model, showing that drag introduces predictable corrections to flight time and trajectory shape, which can be compensated through small adjustments in launch parameters while preserving rhythmic stability. The results bridge classical mechanics, nonlinear dynamics, and human motor control, providing a transparent and physically grounded explanation for the emergence and persistence of stable rhythmic throwing patterns. The model offers a scalable theoretical foundation for understanding coordinated human object interaction in rhythmic tasks.

RECOMMENDATIONS

Based on the findings of this study, several directions for future research are recommended:

Experimental Validation: Controlled laboratory experiments measuring flight times, release timing, and launch variability in human jugglers should be conducted to quantitatively validate the predicted tolerance bounds and synchronization conditions.

Inclusion of Stochastic Motor Noise: While the present analysis accounts for variability through tolerance margins, future work could incorporate explicit stochastic perturbations to model neuromotor noise more directly and assess its impact on long term stability.

Three-Dimensional Extensions: Extending the framework to three-dimensional motion would allow investigation of more complex juggling patterns, including crossing trajectories and spatial asymmetries.

Nonlinear and Quadratic Drag Effects: Further refinement of the aerodynamic model, particularly for higher Reynolds numbers, could improve accuracy for different ball sizes and throwing speeds.

Applications to Robotics and Rehabilitation: The rhythmic and modular structure revealed by the model may inform the design of robotic juggling systems and contribute to rehabilitation strategies that exploit rhythmic coordination for motor learning.

Conflict of Interest: The author declared that there is no conflict of interest

REFERENCES

[1] Bradshaw, J. L. Projectile Motion with Quadratic Drag. American Journal of Physics 91, 258–263 (2023). DOI: 10.1119/5.0095643.

[2] Said, A. A.; Mbewe, H. P.; Mgimba, M. M.; Namanolo, H. S.; Rashid, S. M.; Ussi, S. Mass Dependent Computational Analysis of Projectile Motion under Quadratic Air Drag Using the Runge–Kutta Method. Open Journal of Applied Sciences 15, 4023–4042 (2025). DOI: 10.4236/ojapps.2025.1512260.

[3] Jobunga, E. O.; Warui, K.; Menge, B. K.; Mugambi, E.; Dillmann, B. Analytical Solution of the Projectile Motion Under a Linear Drag Force. Journal of Applied Mathematics (2024). DOI: 10.1155/2024/8881003.

[4] Kovačević, M.; Kuzmanović, L.; Milošević, M. An Experiment for the Study of Projectile Motion. Revista Mexicana de Física E 21, 020217 (2024). DOI: 10.31349/revmexfise.21.020217.

[5] Geller, Noga; Moringen, Alexandra; Friedman, Jason. *Learning Juggling by Gradually Increasing Difficulty vs. Learning the Complete Skill Results in Different Learning Patterns.* Frontiers in Psychology (2023). DOI: 10.3389/fpsyg.2023.1284053

[6] Yamamoto, Koji; Mitoma, Hiroaki; Okada, Mitsuru. *Differences in Anchoring Strategy Underlie Coordination during Three-Ball Juggling Tasks.* Human Movement Science (2021). DOI: 10.1016/j.humov.2021.102678

[7] Nickl, Robert W.; Daniels, Garrett L.; Sternad, Dagmar. *Complementary Spatial and Timing Control in Rhythmic Arm Tasks.* Journal of Neurophysiology (2019). DOI: 10.1152/jn.00194.2018

[8] Huys, Raoul; Beek, Peter J.; van Santvoord, A. A. M. *Multiple Time Scales and Multiform Dynamics in Learning 3-Ball Cascade Juggling.* Journal of Experimental Psychology: Human Perception and Performance 30, 665–681 (2004). DOI: 10.1037/0096-1523.30.4.665

[9] Yamamoto, K. Attractor Stability in Coordination Patterns of Expert Jugglers. Scientific Reports (2020). DOI: 10.1038/s41598-020-60066-7.

[10] Zago, M.; Lacquaniti, F. Multi-Segmental Movement Patterns Reflect Rhythmic Coordination in Juggling. Human Movement Science (2017). DOI: 10.1016/j.humov.2017.01.002.

[11] Putnam, C. A. Sequential Motions of Body Segments in Throwing Skills. Journal of Biomechanics 26, 125–135 (1993). DOI: 10.1016/0021-9290(93)90084-R.

[12] Nasution, B. Basic Mechanics of Lagrange and Hamilton as Reference. Journal of Physics: Conference Series (2023). DOI: 10.1088/1742-6596/2920/1/012345.

[13] Nie, J.-M.; Liu, X.-B.; Zhang, X.-L. An Integrated Lagrangian Modeling Method for Mechanical Systems with Memory Elements. Machines 12, 208 (2024). DOI: 10.3390/machines12030208.

[14] Lagrangian approaches to dynamic coordination and control. **International Journal of Nonlinear Mechanics** (2024).

[15] Abu Salem, K. The Key Role of Research in Flight Dynamics, Control, and Simulation for Advancing Aeronautical Sciences. Aerospace 11, 734 (2024). DOI: 10.3390/aerospace11090734.

[16] Motor Control Beyond Reach: How Humans Hit a Target with Rhythmic Coordination. Royal Society Open Science (2022). DOI: 10.1098/rsos.220581.

[17] Dynamics of projectile motion with Newton drag and analytic solutions. **Physics of Fluids**, **36**, 012001 (2024).

[18] Nicholas N. Topman, G.C.E Mbah and VE Asor (2025). Mathematical Model on Dimensional Analysis of Stratified Deep Water Equations under Modified Gravity and Coriolis Effect to Obtain Reynolds Number. Journal of the Nigerian Association of Mathematical Physics. https://doi.org/10.60787/jnamp.vol71no.627

[19] Nicholas N. Topman (2026). Mathematical Model on impact of Reynolds number on cascading balls. International Journal of Development Mathematics. https://doi.org/10.62054/ijdm/0301.09